Available online at www.sciencedirect.com

ScienceDirect

Physics Procedia 66 (2015) 242 – 248

Physics Procedia

C 23rd Conference on Application of Accelerators in Research and Industry, CAARI 2014

Neutron Imager and Flux Monitor Based on Micro Channel Plates (MCP) in Electrostatic Mirror Configuration

V. Variale[a,]*

[a]*Istituto Nazionale Fisica Nucleare,INFN Sezione di Bari, Italy*

Abstract

In this paper, a new high transparency device based on MCP for the monitoring the flux and spatial profile of a neutron beam will be described. The assembly consists of a carbon foil with a 6Li deposit, placed in the beam, and a MCP equipped with a phosphor screen readout viewed by a CCD camera, placed outside the beam. Secondary emitted electrons (SEE) produced in the carbon foil by the alpha-particles and tritons from the 6Li+n reaction, are deflected to the MCP detector by means of an electrostatic mirror, suitably designed to preserve the spatial resolution. The conductive layer on the phosphor can be used for neutron counting, and to obtain time-of-flight information.

A peculiar feature of this device is that the use of an electrostatic mirror minimizes the perturbation of the neutron beam, i.e. absorption and scattering. It can be used at existing time-of-flight (TOF) facilities, in particular at the n_TOF facility at CERN, for monitoring the flux and special profile of the neutron beam in the thermal and epithermal region.

In this work, the device principle and design will be presented, together with the main features in terms of resolution and neutron detection efficiency.

Selection and peer-review under responsibility of the Organizing Committee of CAARI 2014

Keywords: neutron detection, beam monitor

1. Introduction

In the last years, Micro Channel Plates (MCP) devices have been largely employed both for detection of ionizing radiation and as image intensifier (infrared range). It has also been demonstrated that MCPs can be applied in neutron detection and imaging with many advantages. The use of MCP for neutron detection was proposed for the first time in 1987 at Los Alamos [1] for fast neutrons. More recently, MCP have been proposed as thermal neutron detectors, combined with a suitable converter [2,3].

* Corresponding author. Tel.: +390805442344; fax: +390805443190
E-mail address: incenzo.variale@ba.infn.it

Selection and peer-review under responsibility of the Organizing Committee of CAARI 2014
doi:10.1016/j.phpro.2015.05.031

The Micro Channel Plates (MCP), originally developed as an amplification element for image intensification devices by Wiza (1979), consists of a two-dimensional array of many microscopic glass capillaries (channels) which are fused together and sliced in the shape of a thin disk or rectangle. The internal wall of each channel is processed to forming an independent Secondary Electron (SE) multiplier.

In the last years, MCP devices have been largely employed as both detectors of ionizing radiation and image intensifiers. It has also been demonstrated that MCPs can be applied in neutron detection and imaging with many advantages. The use of MCP for fast neutron detection was proposed for the first time in 1987 at Los Alamos by MacArthur (1987). In these experiments polyethylene layers were used before the MCP in such a way that the recoil protons produced by fast neutron could be detected.

Years later, MCP devices doped by ^{10}B have been proposed and then designed as thermal neutron detectors by Frazer and Pearson (1990), Siegmund et al. (2001) and Tremsin et al. (2005). These kind of detectors, however, did not reach a very high neutron detection efficiency (about 21%) since the doping concentration was limited by the production process of the MCP glass. More recently, in order to increase that efficiency a ^{nat}Gd coating on the MCP channel inner wall has been proposed and studied by Lu et al. (2012). The Atomic Layer Deposition (ALD) technique has been used for inner wall coating and a $^{nat}Gd_2O_3$ film of about 100 nm has been deposited. In that paper, simulation results show that detection efficiency about 70% could be reached for 25.3 meV neutrons .

In this work a new high transparency device based on MCP for monitoring the flux and spatial profile of a neutron beam will be described. The device consists of a carbon (C) foil with a ^6Li deposit that are placed in the neutron beam, and a phosphor screen with a coupled CCD camera placed out of the beam. Secondary electrons (SE) produced in the C foil by the α-particles and tritons emitted as result of the ^6Li+n reaction, are deflected towards the MCP detector by means of an electrostatic mirror designed to preserve the spatial resolution of the beam image. Furthermore, the conductive layer on the phosphor can be used for neutron counting and for time-of-flight measurements.

A peculiar feature of this device is that the use of an electrostatic mirror minimizes the perturbation of the neutron beam, i.e. absorption and scattering. It can be used at existing time-of-flight facilities, in particular in the n_TOF (neutron Time Of Flight) facility at CERN, for monitoring the flux and spatial profile of the neutron beam in the thermal and epithermal energy regions.

The MCP devices have many advantageous detection features [Hamamatsu (2013)] as: fast time response (signal rise time about 300 ps); low dead time (for a diameter channel of 6μm about 100 ns); high counting rate (more than 10^8 sec^{-1}); low dark current (for a vacuum better than 10^{-6} mb 1Hz/cm^2); and a very high spatial resolution (6 μm per 1-stage MCP and 25 μm per 2-stage MCP, the chevron configuration). This last feature make the MCP very suitable to be used in beam monitor device construction. The MCP radiation detection efficiency depends on the radiation type and energy. For electrons in the energy range of 1÷ 2 keV it can reach a maximum value of 85%, for neutrons, on the other hand, it is very low (up to 0.6 % for fast neutrons). For that reason it is necessary of using a converter material to increase the MCP neutron detection efficiency.

2. Beam monitor design

In all mentioned MCP applications as a neutron beam monitor the device was placed directly in the beam. This configuration, depending on their detection efficiency, can substantially perturb the neutron beam which has to be monitored. To minimize those perturbations the detection and readout system should be moved off the beam axis. In order to accomplish to this requirements the MCP-based detection technique with an electrostatic mirror is proposed. An arrangement of this type of beam profile monitor is shown in Fig. 1. The C foil with the converter material, ^6Li in our case, is placed in a plane perpendicular to the neutron beam axis. Since the $^6Li(n,\alpha)t$ reaction, has a cross section of about one thousand of barn for thermal neutrons, α and t ions with energy 2 MeV and 2.7 MeV are produced, respectively. At those energies the α and the t particle ranges, in the C foil, are of 5 and 30 μm, respectively. Then, if we assume a C foil of 20μg/cm^2, which has a thickness of 9 μm, all the α–particles will be stopped and almost all the tritons will pass through the foil. The C foil will emit SE (Secondary Electrons) which will be accelerated by the nearby grid and then driven towards the MCP by the reflecting grids placed at a 45° angle, as shown in the Fig.1 (the electrostatic mirror). The SE impinging on the MCP inner channel wall will generate an

electron avalanche. Behind the MCP (in a chevron configuration) the signal read-out system a phosphor screen followed by a CCD camera, in our design, ensures that a beam image is recorded.

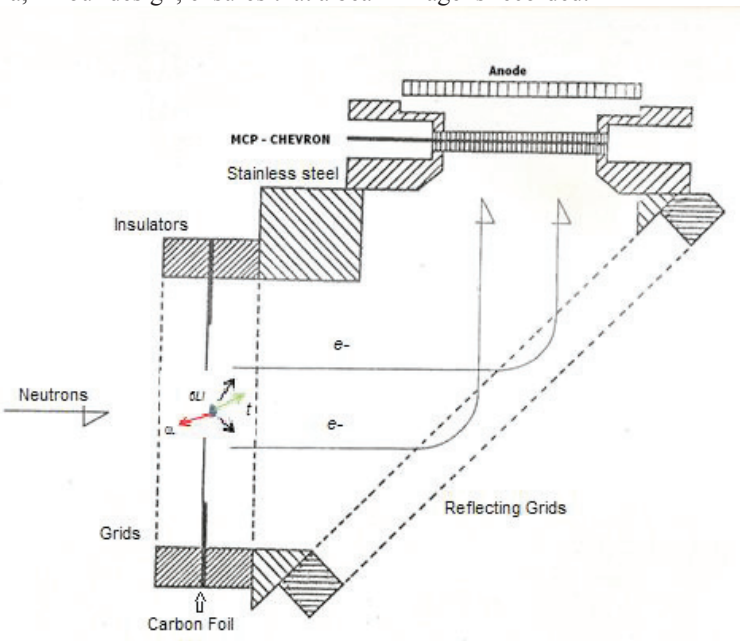

Fig. 1. Scheme of neutron beam monitor with electrostatic mirror configuration. A carbon foil with a deposit of the converter material, ^{6}Li is inserted in the neutron beam, while the electrostatic mirror deflects secondary electrons towards the MCP placed outside the beam.

In the case only a very fast neutron counting is of interest but no beam profile measurements a simple anode could be used, as shown in Fig.1.

It should be noted that as the electrostatic mirror configuration used in Fig. 1 allows for production of a representative image of the neutron beam with minimal perturbation of the flux. This feature is important for neutron facilities but could also serve other purposes.

A good beam monitor must have enough high particle detection efficiency and high spatial resolution. In principle, a large number of neutron interactions is needed to obtain a perfect neutron beam image.

Since the electron detection efficiency in the energy range of 1 ÷ 2 keV for the MCP devices is about 85%, the neutron detection efficiency will depend essentially on the cross section of the reaction used for the neutron conversion (^{6}Li(n,α)t in our case) and on the thickness of a conversion layer. An approximate evaluation of the number of detected neutrons can be done by considering that Lithium has a density of 0.534 g/cm^3 (corresponding to 5.36x10^{23} atoms/cm^3 of ^{6}Li) and that the capture yields (Y) of the reaction in the case of $N\sigma_t \ll 1$ (σ_t is the total microscopic cross section, N is the number of atoms per barn) can be expressed as: $Y \approx [1-(1-N\sigma_t)]\sigma_c/\sigma_t$ (σ_c is the capture cross section). Then, the neutron capture reaction rate is given by $\sigma_c n \Phi_n$ (Φ_n neutron flux). Here the neutron flux of the CERN n_TOF facility at CERN has been considered. That neutron beam is produced for 'spallation' process by 20 GeV protons impinging a target of Lead. It has a broad energy range (from thermal to 1 GeV neutrons). Since the cross section of the conversion reaction is strongly dependent on the neutron energy, it is difficult to evaluate the neutron counting rate expected with the device presented here. For that purpose we carried out a Monte Carlo simulation with the MCNPX code. Fig. 2 shows a simple geometry used in that simulation together with the results on neutron count-rate obtained as a function of the ^{6}Li deposit thickness. The following parametershas been used in the simulations: r = 2 cm (C foil disk radius); l_1 = 1, 2, 3, 4, 5 μm (^{6}Li deposit depth); l_2 = 9 μm (C foil thickness); d = 4 cm (neutron flux diameter); N_t is the number of tritons exiting from C foil towards the electrostatic mirror.

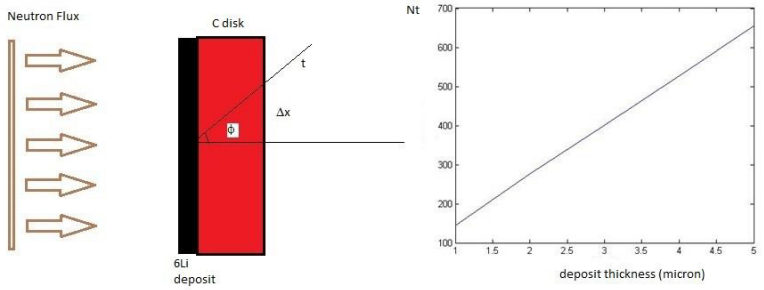

Figure 2. MCNPX simulation geometry. On the left, the simulation results are shown as Nt, the number of tritons exiting from the C foil, *vs* the deposit thickness. Δx indicates the triton position shift at the C foil exit with respect to the capture reaction original position.

The graph shown in Fig. 2 has been obtained normalizing the MCNPX results to the CERN n_TOF neutron source. For a deposit depth of about 3 μm, taking in to account the MCP detection efficiency (85%) a count rate of a few hundred events per proton pulse could be obtained, which is typically sufficient for measuring a beam profile in a relatively short time of a few hours.

The MCP devices have a very good intrinsic spatial resolution (approximately 25 μm in a chevron configuration). If the electrostatic mirror does not cause any deformation of the neutron beam image on the MCP input surface, this monitor could reach the maximum intrinsic resolution of the MCP. Unfortunately, we can foresee two sources of error in the neutron position determination:

(1) the source of error that is related to the angle of emission of the triton, which could then exit from the C foil at a position different relative to where neutron capture occurred inside the C foil (Δx, see Fig. 2);
(2) the error due to SE initial conditions (such as the initial kinetic energies and emission cone angle) which could cause deviations from the expected mirror trajectories. The following considerations apply to these problems:

(1) As shown in Fig.2, Δx is the shift due to the capture reaction emission angle Φ. Evaluation of Δx can be done considering the thickness of the C foil. If we assume a C foil thickness of about 9 μm and a depth of the ^{6}Li deposit of 2 μm, since $\Delta x = d\ \mathrm{tg}\Phi$, Δx values lower than ±60 μm can be obtained for an emission cone angles Φ lower than 80°. If we consider $\Phi < 85°$ we would get a maximum error detection, Δx, lower than ±100 μm. One can notice that for the isotropic capture reaction and the triton having a flat emission angle distribution at low neutron energies, the fraction of the tritons emitted in the electrostatic mirror direction with a Δx lower than 60 μm (corresponding to a Φ<80°) is about 90%.
(2) According to Billeband et al. (1997), Nickles et al. (1998), Rothard and Gervais (2006), the SE emission initial conditions can be summarized as follows:

a) the yield depends, in general, on the stopping power of the incident radiation;
b) the forward SE emission can be greater than the backward one by a factor 1.55;
c) the SE energy distribution is, in general, peaked around few eV;
d) when a negative bias is applied to the emitting surface, the SE emission cone angle (Φ) can be reduced at values < 10°.

To study the beam image reproduced on the MCP input surface, simulations of the SE trajectories in the electrostatic mirror have been carried out with the SIMION code.. Further SE trajectories simulations have been performed to study the influence of the SE initial conditions on the beam image quality.

In Fig.3a, eight equidistant SE trajectories are shown starting from the C foil surface with a *dy* distance between them. The green line trajectory of the *i_th* SE has initial conditions: y_i is the position along y-axis; the initial kinetic energy $E_{ki} = i$ eV with i =1, ..,8; the initial emission cone angle Φ_i=0°. The SE final positions along the x-axis are indicated with x_i. In the simulation results of Fig.3a, it can be noticed that the SE trajectories maintain their relative

distance at the end points on the MCP input surface ($dx = dy$). One can conclude that the initial conditions used for the 'green' SE generate an image on the MCP (along the x axis) which is nearly identical to the object along the y axis. On the contrary, the blue line trajectories of Fig. 3a indicating the SE starting with the same initial positions along the y axis but with different initial kinetic energies (E_{ki}= 4 eV) and emission cone angles (Φ_i= 6°, 8° up to 20°) produce a deformed image . The SE final positions in this case, in fact, are indicated by x_i' instead of x_i, with the quantity $\delta x = x_i' - x_i$ defined as the 'deformation' parameter. It can be noticed again in Fig.3a that the blue SE final positions, x_i', can be sensitively different from the x_i (the green line final positions). The deformation parameter of up to 80% can be reached with a Φ_i of about 20°.

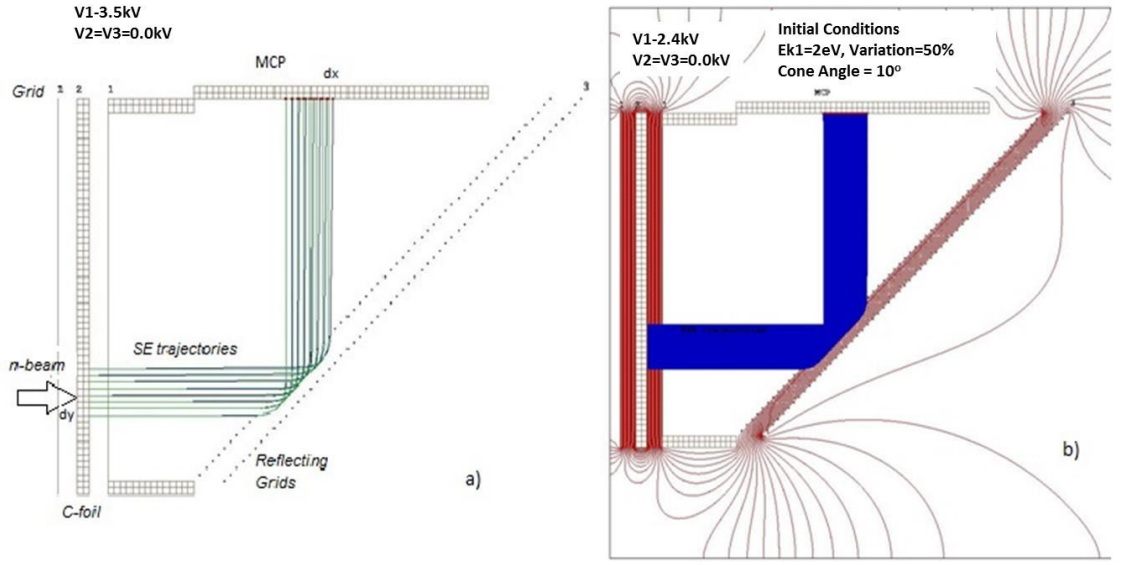

Figure 3. a) SE trajectories simulations in the electrostatic mirror. The eight SE start from the C foil at equidistant positions, y_i: the green trajectories have the following SE initial conditions , E_k= 1 eV and Φ= 0°; the blue trajectories: E_k =2 eV, Φ= 10°; b) large number of SE trajectories with a flat distribution of the initial conditions (E_{ki}= 2 eV ± 50% and with Φ_i < 10°). The red lines indicate equipotential lines.

Many further simulations have been carried out combining several changes of E_{ki} and Φ_i to evaluate their effect on the $\delta x'$ values. As an example, simulation results with the SE initial conditions E_{ki}= 2 eV and Φ_i < 10° give a maximum $\delta x'$ value of 10%. Those initial condition values, as discussed in (2), can be considered realistic SE initial conditions.

Further simulations with a large number of SE trajectories having a flat distribution on the initial conditions have been also performed. In Fig. 3b, the case with E_{ki}= 2 eV ± 50% (as the maximum variation) and $\Phi_i \leq 10°$ is shown. In that case the average value $\delta x'$ of about 6% has been estimated.

3. Monitor prototype production

The development of the monitor prototype is underway. An MCP with the phosphor screen assembly have been mounted on a vacuum flange (Hamamatsu F6959). The P47 phosphor is used in this device. It has a very short afterglow time of 0.11 μs and a light emission of about 430 nm. A CCD camera that has its sensitivity in the same wavelength range is required for the light signal acquisition, such as the Kodak KAF-1400 type which has a high sensitivity in the range 400÷1000 nm. Furthermore, a vacuum chamber is needed since the MCP operates in high vacuum. Fig. 4a shows the chamber designed for this purpose. The MCP assembly is mounted on the top flange of the vacuum chamber. In the present design, the MCP is placed at about 8 cm from the electrostatic mirror, aligned

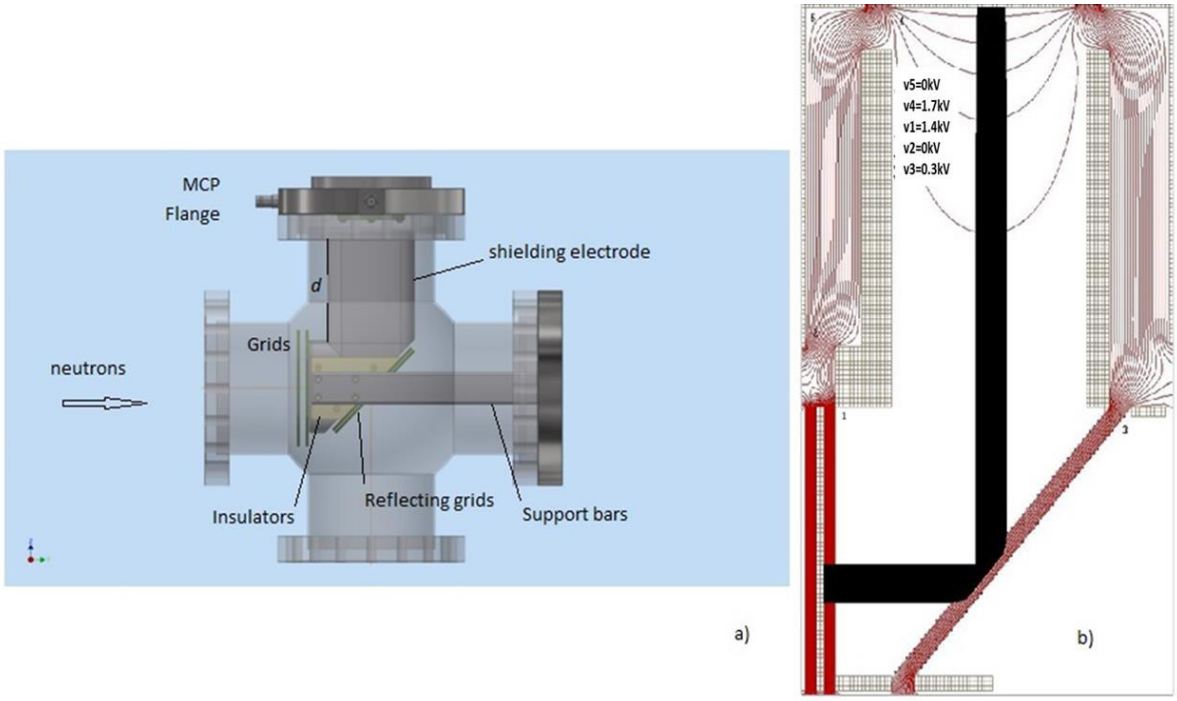

.Figure 4. a) Drawing of the modified electrostatic mirror inside the cross shaped vacuum chamber; b) Results of the SE trajectories simulation for the modified electrostatic mirror. The use of the electrostatic lens avoid beam profile image enlargements due to SE divergent trajectories. The voltage applied on the electrodes are shown on figure. The red lines indicate equipotential lines

with the beam axis. Consequently, secondary electrons have to follow longer trajectories in this configuration. Further simulations of the SE behavior have been carried out to verify the effect of the geometry on the beam image. Further simulations of the SE behavior have been carried out to verify the effect of the geometry on the beam image. The results of simulations have shown that a shielding electrode is needed because the vacuum chamber wall is at the ground (see Fig.4b). Furthermore, since the SE now travel a longer path (d=8cm), their initial trajectory divergence, even small, contributes to enlarge the beam profile image.

However, this effect can be reduced by applying a proper potential difference between the shielding electrode and the MCP input surface. The simulation results of fig. 4b) show how that electrostatic lens before the MCP practically cancel out the beam spot image enlargement due to SE divergent trajectories.

4. Conclusions

A new type of a neutron beam monitor of high transparency which minimizes perturbations of neutron beam is presented. The device uses an MCP coupled with a phosphor screen and an electrostatic mirror that reflects the neutron beam spot image, produced by an appropriate converter, on a plane off the beam axis.

Computer simulations show that this monitor could provide a very good spatial resolution (up to few hundreds of microns) and a good detection efficiency which can be enhanced by increasing the ^{6}Li-deposit thickness. The detection efficiency could allow a counting rate of hundreds of neutrons per pulse in the case of the CERN n_TOF facility.

The device is currently under development. It is planned to be tested at the CERN n_TOF facility in the next year.

Acknowledgements

The author would like to thanks Dr. N. Colonna for his valuable suggestions and Mr. V. Valentino for mechanical drawing.

References

Wiza, J., 1979. Nucl. Instr. & Meth. 162, 587.
Fraser,G., Pearson, J., 1990. Nucl. Instr. & Meth. A293,569.
O. H. W. Siegmund, A. S. Tremsin, J. V. Vallerga, J. Hull, IEEE Trans. Nucl.Sci. NS-48 (2001) 430.
A. S. Tremsin, W. B. Feller, R. G. Downing, , Nucl. Instr. And Meth. A539 (2005) 278.
Nianhua Lu, Yigang Yang, Jingwen Lv, Jingshen Pan, Manchun Liang Yuanjing Li, Physics Procedia 26 (2012) 61.
Hamamatsu MCP guide, Technical information (2013).
A. Billebond et al., "Ion by ion measurements secondary electron emission of carbon foils under the impact of MeV H+, H0, H- projectiles" Phys.Rev. A vol. 55, N.2 Feb. (1997).
N. Nickels, R. E. Davies and J. R. Dennison, Applications of Secondary Electron Energy and angular distribution to space Charging", 6th SPACE CHARGING CONFERENCE, AFRL-VS-TR, 20001578 (1998).
H. Rothard and B. Gervais, "Electron Emission from Solids Irradiated with Swift Ion Beams", in ION BEAM SCIENCE; Solved and unsolved problems, Ed. By P. Sigmund, Royal Danish Academy of Scienc and Letters, Copenhagen (2006).